

A PHYSICAL MODEL FOR ACTIVE GALACTIC NUCLEI WITH DOUBLE-PEAKED BROAD EMISSION LINES

XINWU CAO^{1,3} AND TING-GUI WANG^{2,3}*accepted by ApJ*

ABSTRACT

The double-peaked broad emission lines are usually thought to be linked to accretion disks, however, the local viscous heating in the line-emitting disk portion is usually insufficient for the observed double-peaked broad-line luminosity in most sources. It was suggested that the X-ray radiation from an ion-supported torus in the inner region of the disk can photo-ionize the outer line-emitting disk region. However, our calculations show that only a small fraction ($\lesssim 2.3$ per cent) of the radiation from the radiatively inefficient accretion flow (RIAF) in the inner region of the disk can photo-ionize the line-emitting disk portion, because the solid angle of the outer disk portion subtended to the inner region of the RIAF is too small. We propose a physical model for double-peaked line emitters, in which only those AGNs with sufficient matter above the disk (slowly moving jets or outflows) can scatter enough photons radiated from the inner disk region to the outer line-emitting disk portion extending from several hundred to more than two thousand gravitational radii. Our model predicts a power-law r -dependent line emissivity $\epsilon^{\text{H}\alpha} \propto R_d^{-\beta}$, where $\beta \sim 2.5$, which is consistent with $\beta \sim 2-3$ required by the model fittings for double-peaked line profiles. Using a sample of radio-loud AGNs with double-peaked emission lines, we show that the outer disk regions can be efficiently illuminated by the photons scattered from slow or mild relativistic electron-positron jets with $\gamma_j \lesssim 2$. It is consistent with the fact that no double-peaked emission line is present in strong radio quasars with relativistic jets. For radio-quiet double-peaked line emitters, slow outflows with Thomson scattering depth ~ 0.2 instead of jets can scatter sufficient photons to (illuminate) the line-emitting regions. This model can therefore solve the energy budget problem for double-peaked line emitters.

Subject headings: galaxies: active—quasars: emission lines—accretion, accretion disks

1. INTRODUCTION

Only a small fraction of active galactic nuclei (AGNs) exhibit double-peaked broad-line profiles, for example, the largest sample available so far is the 116 double-peaked Balmer line AGNs, which are found from an initial sample consisting of 5511 broad line AGNs with $z < 0.5$ observed by the Sloan Digital Sky Survey (SDSS) (Strateva et al. 2003). Some previous authors mainly focused on the double-peaked broad lines in radio-loud (RL) AGNs (e.g., Perez et al. 1988; Chen et al. 1989; Chen & Halpern 1989; Eracleous & Halpern 1994, 2003). A complete survey on RL AGNs finally resulted in 20 double-peaked line emitters (Eracleous & Halpern 1994, 2003). It is still a mystery why (only) a small fraction of AGNs exhibit double-peaked broad-line profiles.

Some different scenarios were suggested for the origin of double-peaked emission lines, namely, (1) emission from the accretion disk (e.g., Chen et al. 1989; Chen & Halpern 1989), (2) emission from a binary broad-line region (BLR) in a binary massive black hole system (e.g., Gaskell 1983, 1988), (3) emission from the bipolar outflows (e.g., Zheng et al. 1990), (4) emission from a spherically symmetric BLR illuminated by an anisotropic ionizing radiation source (e.g., Goad & Wanders 1996). The accretion disk model is the most favorable one among them (see detailed comparison between these different scenarios in Eracleous & Halpern 2003, and references therein). The widths of double-peaked

lines range from several thousand to nearly 40000 km s⁻¹ (e.g. Wang et al. 2005). In the accretion disk model, the double-peaked emission lines are radiated from the disk region between around several hundred gravitational radii to more than two thousand gravitational radii, and their profiles can be well fitted by the accretion disks with a power-law line emissivity (e.g., Chen et al. 1989; Chen & Halpern 1989; Eracleous & Halpern 2003). However, none of these scenarios can answer why only a small fraction of AGNs have been detected as double-peaked line emitters. For example, in the accretion disk model, one may expect to observe double-peaked lines in most AGNs, as the AGNs with higher inclination angles have more chances to be observed, until their accretion disks are obscured by the putative tori (e.g., Antonucci 1993), if the orientations of AGNs are isotropically distributed in space. Another difficulty for the disk model is the “energy budget” problem, i.e., the local viscously dissipated power in the line-emitting disk portion is usually insufficient for the observed double-peaked broad-line luminosity in most sources, and the temperatures of the line-emitting disk regions are too low to produce the observed H_α lines (Chen et al. 1989; Chen & Halpern 1989; Eracleous & Halpern 1994, 2003). The X-rays from a hot ion-supported torus in the inner disk region are assumed to irradiate the outer line-emitting disk region and then to solve the “energy budget” problem (e.g., Chen & Halpern 1989).

We discuss the illumination of the outer disk regions by the inner ion-supported tori in §2. In this paper, we suggest a physical model for these double-peaked line emitters. In this model, a fraction of photons from the accretion disk are scattered by the electrons in the jet/outflow back to photo-ionize the outer line-emitting region, and then to produce the observed emission lines. We describe our model in

¹ Shanghai Astronomical Observatory, Chinese Academy of Sciences, 80 Nandan Road, Shanghai, 200030, China; cxw@shao.ac.cn

² Center for Astrophysics, University of Science and Technology of China, Hefei 230026, China

³ Joint institute for Galaxy and Cosmology, Chinese Academy of Sciences, China

§3. The cosmological parameters $\Omega_M = 0.3$, $\Omega_\Lambda = 0.7$, and $H_0 = 70 \text{ km s}^{-1} \text{ Mpc}^{-1}$ have been adopted in this work.

2. ION SUPPORTED HOT TORI IN DOUBLE-PEAKED LINE EMITTERS

The putative hot ion supported tori in double-peaked line emitters are well modelled by the advection dominated accretion flows (ADAFs, old version of RIAFs) (Narayan & Yi 1994, 1995). The RIAF can survive only if its accretion rate \dot{m} ($\dot{M}/\dot{M}_{\text{Edd}}$) is less than a critical value \dot{m}_{crit} , which is a function of the viscosity parameter α (e.g., Narayan & Yi 1995). The three-dimensional MHD simulations suggest that the viscosity parameter α in the accretion flows is ~ 0.1 (Armitage 1998), or $\sim 0.05 - 0.2$ (Hawley & Balbus 2002). For some double-peaked line emitters, their bolometric luminosities could be as high as one-tenth of the Eddington value. Their X-ray luminosities $L_X^{0.1-2.4\text{keV}}$ could be as high as $10^{43-44} \text{ ergs s}^{-1}$ for the double-peaked line emitters with black hole masses of $10^{7-9} M_\odot$ (e.g., Table 7 in Eracleous & Halpern 2003, and Table 1 in this paper). The maximal X-ray luminosity for a RIAF surrounding a massive black hole can be calculated based on the global solution for the RIAF. Adopting $\dot{m}_{\text{crit}} = 0.01$, corresponding to $\alpha \simeq 0.2$, which is a conservative choice, we can calculate the global structure of the RIAF. For such a RIAF accreting at the critical rate, its X-ray luminosity $L_X^{0.1-2.4\text{keV}} = 7.3 \times 10^{40} \text{ ergs s}^{-1}$ for a $10^8 M_\odot$ black hole (see Manmoto 2000; Cao 2005, for detailed description of the calculation on the flow structure). The X-ray luminosity of the RIAF depends almost linearly on the black hole mass while \dot{m} is fixed. For some X-ray luminous double-peaked line emitters, a very high viscosity $\alpha \sim 1$ is required for the presence of RIAFs in these sources, which is in contradiction with the MHD simulations.

It is well known that most gravitational energy of accretion matter is released in a small region close to the black hole, either for a standard thin disk (Shakura & Sunyaev 1973) or a RIAF. In Fig. 1, we calculate the ratio $L_{\text{RIAF}}(< R_d)/L_{\text{RIAF}}^{\text{tot}}$ as a function of R_d based on the global RIAF structure (Cao 2005; Manmoto 2000). It is found that more than 70 per cent radiation is from the region within $0.3 R_{d,\text{tr}}$, where $R_{d,\text{tr}}$ is the radius of the RIAF connecting to the outer standard thin disk. Assuming homogeneous distribution of the gases in z -direction of the RIAF, our calculation shows that less than 2.3 per cent radiation from the RIAF in the inner region of the disk can illuminate the line-emitting disk region with $R_d > R_{d,\text{tr}}$, because the solid angle of the outer disk portion subtended to the inner region of the RIAF is too small. For more realistic z -direction density distribution of the RIAF, the gases are denser in the midplane of the flow and the resulted fraction should even be less than this value. Thus, the hot ion-supported tori are unable to heat the outer line emitting disk regions efficiently for most double-peaked line emitters, even if the observed luminous X-ray emission can be attributed to hot ion-supported tori.

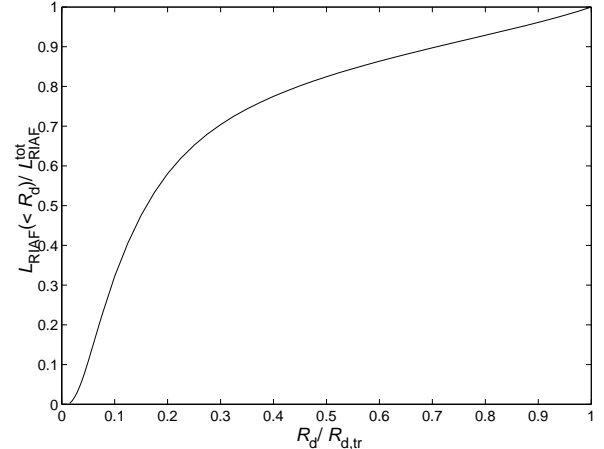


FIG. 1.— The ratio $L_{\text{RIAF}}(< R_d)/L_{\text{RIAF}}^{\text{tot}}$ as a function of $R_d/R_{d,\text{tr}}$.

3. THE MODEL

In this paper, we employ the inhomogeneous conical jet model (see Königl 1981, for details), which can successfully explain most observational features of radio-loud AGNs (e.g., Jiang et al. 1998). For a free jet, its half-opening angle $\phi_j = 1/\gamma_j$ (Blandford & Königl 1979; Hutter & Mufson 1986), where γ_j is the Lorentz factor of the jet. The non-thermal electrons in the jet is described by a power-law energy distribution,

$$n_e(r_j, \gamma_e) = n_{e,0}(r_j) \left(\frac{\gamma_e}{\gamma_{e,\text{min}}} \right)^{-(2\alpha_e+1)}, \quad (1)$$

from $\gamma_{e,\text{min}}$ to $\gamma_{e,\text{max}}$ (Königl 1981). In Königl's jet model, the jet is assumed to move at a constant velocity, which is a good approximation, though the dynamics of electron-positron jets is very complicated (e.g., Renaud & Henri 1998). For simplicity, we adopt a conventional assumption of the jet moving at a constant velocity $\beta_j c$.

It is still unclear for the jet composition, i.e., electron-positron or electron-proton (see Worrall & Birkinshaw 2004, for a recent review and references therein). For an electron-proton jet, the lower limit of electron Lorentz factor $\gamma_{e,\text{min}}$ is required to be greater than 100, while $\gamma_{e,\text{min}}$ could be as low as unity for an electron-positron jet (e.g., Celotti & Fabian 1993). This is consistent with the detection of circular polarization, which strongly suggests that the jets are electron-positron plasmas and have low $\gamma_{e,\text{min}} \lesssim 10$ (e.g. Wardle et al. 1998). The similar conclusion is arrived from powerful large scale X-ray jets, if they are interpreted as inverse-Compton scattering of cosmological microwave background photons in fast jets. The typical energy of the photons radiated from the standard thin accretion disk surrounding a massive black hole is $\nu_d^* \sim 10 \text{ eV}$. The soft photons from such a standard disk are Compton up-scattered to the hard X-ray band ($\gtrsim 10 \text{ keV}$, or even γ -ray bands) for an electron-proton jet, because $\gamma_{e,\text{min}} \sim 100$. These hard X-ray photons can hardly photoionize the outer line-emitting disk region. If a thermal electron population with similar density co-exists with the non-thermal power-law electrons in the relativistic jet, the soft X-ray photons scattered by the thermal electrons in the jet can ionize the disk. Such thermal plasmas in a relativistic jet may produce significant Doppler shifted emission or absorption lines depending on their temperature, which seems inconsistent with observations. Thus, we will not consider this possi-

bility in this work, though the presence of thermal electrons in the jet cannot be ruled out. The situation is different for the electron-positron jet, of which $\gamma_{e,\min} \sim 1$. Most Compton scattered photons by the electrons in electron-positron jets are in soft X-ray bands, which can efficiently photo-ionize the line-emitting disk region, so we will focus on the electron-positron jets hereafter in this work.

The kinetic luminosity of a relativistic moving electron-positron jet with Lorentz factor γ_j is

$$\begin{aligned} L_{\text{kin}} &= \dot{M}_{\text{jet}}(\gamma_j - 1)c^2 + \dot{M}_{\text{jet}}2\alpha_e \gamma_{e,\min}^{-1} \left[1 - \left(\frac{\gamma_{e,\min}}{\gamma_{e,\max}} \right)^{2\alpha_e} \right]^{-1} \\ &\times \int_{\gamma_{e,\min}}^{\gamma_{e,\max}} \left(\frac{\gamma_e}{\gamma_{e,\min}} \right)^{-(2\alpha_e+1)} (\gamma_e - 1)c^2 d\gamma_e \\ &\simeq \dot{M}_{\text{jet}}c^2 \left(\gamma_j + \frac{2\alpha_e \gamma_{e,\min}}{2\alpha_e - 1} - 2 \right), \end{aligned} \quad (2)$$

where m_e is electron rest mass, $\gamma_{e,\max} \gg \gamma_{e,\min}$ is assumed, and the mass loss rate of the jet is given by

$$\dot{M}_{\text{jet}} = 2m_e n_e(r_j) 2\pi r_j^2 (1 - \cos \phi_j) R_g^2 \gamma_j \beta_j c. \quad (3)$$

For an accretion disk surrounding a black hole, most gravitational energy is released in the inner region of the disk (within several Schwarzschild radii close to the marginal stable orbit r_{ms} , Shakura & Sunyaev 1973), where r_{ms} is in units of gravitational radius $R_g = GM_{\text{bh}}/c^2$. For simplicity, we use a ring with radius $r_d = 2.25r_{\text{ms}}$, where is the main contribution to the integral disk luminosity (Shakura & Sunyaev 1973), to approximate the accretion disk radiation. The solid angle of the surface of the jet slice between r_j and $r_j + dr_j$ subtended to the accretion disk (ring) with radius r_d is

$$\begin{aligned} \frac{d\Omega(r_j)}{dr_j} \\ = \frac{2\pi r_j r_d \sin \phi_j \cos \phi_j}{[(r_d - r_j \sin \phi_j)^2 + r_j^2 \cos^2 \phi_j] \times [(r_j - r_d \sin \phi_j)^2 + r_d^2 \cos^2 \phi_j]^{1/2}}, \end{aligned} \quad (4)$$

where r_j is the distance from the apex of the jet.

The jet is Compton thin in transverse direction at large radii, while it becomes Compton thick at small radii. We can estimate the transition radius $r_{j,\text{tr}}$ by

$$\tau_{\text{es},\text{tr}}(r_{j,\text{tr}}) = r_{j,\text{tr}} R_g \phi_j n_e(r_{j,\text{tr}}) \sigma_T \sim 1, \quad (5)$$

beyond which the jet becomes Compton thin in transverse direction for electron scattering. Here the Thomson cross-section $\sigma_T = 6.652 \times 10^{-25} \text{ cm}^2$. In the region of the jet with $r_j \lesssim r_{j,\text{tr}}$, the photons from the disk are mostly scattered in a thin layer at the jet surface.

The angle-dependent inverse-Compton scattered photons from the slice of the jet $r_j \rightarrow r_j + dr_j$ measured in the source frame is

$$\begin{aligned} \frac{dN_{\text{Comp}}(r_j, \mu_L)}{dt dr_j d\Omega_{\text{scat}}} &= \frac{f^{\text{IC}} L_{\text{disk}}}{\pi h \nu_d^*} \frac{1 - \beta_j \cos \phi_j}{\gamma_j^2 (1 - \beta_j \mu_L)^3} \\ &\times \frac{1}{2\pi} \frac{r_j \cos \phi_j}{[(r_d - r_j \sin \phi_j)^2 + r_j^2 \cos^2 \phi_j]^{1/2}} \frac{d\Omega(r_j)}{dr_j}, \end{aligned} \quad (6)$$

for the Compton thick part of the jet ($r_j \lesssim r_{j,\text{tr}}$), where $\mu_L = \cos \theta_{\text{scat}}$, and θ_{scat} is the angle of the scattered photons measured from the axis of the jet in the source frame given by

$$\mu_L = -\frac{r_j \cos \phi_j}{[r_j^2 \cos^2 \phi_j + (r_L - r_j \sin \phi_j)^2]^{1/2}}. \quad (7)$$

As only the scattered photons with energy $\geq \nu_{\text{ph}}^{\min} = 13.6 \text{ eV}$ can efficiently photo-ionize the gases in the line-emitting disk region, the correction factor f^{IC} describing the fraction of the scattered photons with energy $\geq \nu_{\text{ph}}^{\min}$ measured in the source rest frame, is given by

$$f^{\text{IC}} = \min \left[\left(\frac{\gamma_{e,\min}'}{\gamma_{e,\min}} \right)^{-2\alpha_e}, 1 \right]. \quad (8)$$

Only the photons scattered by the electrons with $\gamma_e \geq \gamma_{e,\min}'$ are more energetic than 13.6 eV measured in the source frame, so the value of $\gamma_{e,\min}'$ is given by

$$\gamma_{e,\min}' = \max \left[\frac{(1 - \beta_j \mu_L)^{1/2} \nu_{\text{ph}}^{\min 1/2}}{(1 - \beta_j \mu_j^s)^{1/2} \nu_d^{*1/2}}, 1 \right], \quad (9)$$

where

$$\mu_j^s = \frac{r_j - r_d \sin \phi_j}{[r_j^2 \cos^2 \phi_j + (r_d - r_j \sin \phi_j)^2]^{1/2}}. \quad (10)$$

Assuming a line-emitting ring with radii r_L extending from ξ_1 to ξ_2 , we obtain the total photons scattered in the Compton thick jet slice which can photo-ionize the line-emitting disk region,

$$\begin{aligned} \frac{dN_{\text{Comp}}^{\text{line}}(r_j; r_j \leq r_{j,\text{tr}})}{dt dr_j} &= \int_{\mu_{L1}}^{\mu_{L2}} \frac{f^{\text{IC}} L_{\text{disk}}}{\pi h \nu_d^*} \frac{1 - \beta_j \cos \phi_j}{\gamma_j^2 (1 - \beta_j \mu_L)^3} \\ &\times \frac{1}{2\pi} \frac{r_j \cos \phi_j}{[(r_d - r_j \sin \phi_j)^2 + r_j^2 \cos^2 \phi_j]^{1/2}} \frac{d\Omega(r_j)}{dr_j} 2\pi d\mu_L. \\ &= \int_{\mu_{L1}}^{\mu_{L2}} \frac{f^{\text{IC}} L_{\text{disk}}}{\pi h \nu_d^*} \frac{1 - \beta_j \cos \phi_j}{\gamma_j^2 (1 - \beta_j \mu_L)^3} \\ &\times \frac{2\pi r_j^2 r_d \sin \phi_j \cos^2 \phi_j d\mu_L}{[(r_d - r_j \sin \phi_j)^2 + r_j^2 \cos^2 \phi_j]^{3/2} \times [(r_j - r_d \sin \phi_j)^2 + r_d^2 \cos^2 \phi_j]^{1/2}}. \end{aligned} \quad (11)$$

For the jet part with $r_j > r_{j,\text{tr}}$, it is Compton thin for electron scattering. In this case, we have to include radiative transfer of the incident photons in the jet. Similar to Compton thick case, we can derive the inverse-Compton scattered photons from the slice of the jet $r_j \rightarrow r_j + dr_j$ photo-ionizing the line-emitting ring measured in the source frame as

$$\begin{aligned} \frac{dN_{\text{Comp}}^{\text{line}}(r_j; r_j > r_{j,\text{tr}})}{dt dr_j} \\ \simeq \int_{\mu_{L1}}^{\mu_{L2}} \frac{f^{\text{IC}} L_{\text{disk}}}{\pi h \nu_d^*} \frac{1 - \beta_j}{\gamma_j^2 (1 - \beta_j \mu_L)^3} \frac{1}{4\pi} \int_{r_{j,\min}}^{r_j} n_e(r_j) \sigma_T R_g \exp[-\tau_{\text{es}}(r_j, r_j')] \\ \times \frac{2\pi r_j^2 r_d \sin \phi_j \cos^2 \phi_j dr_j' 2\pi d\mu_L}{[(r_d - r_j' \sin \phi_j)^2 + r_j'^2 \cos^2 \phi_j]^{3/2} \times [(r_j' - r_d \sin \phi_j)^2 + r_d^2 \cos^2 \phi_j]^{1/2}}, \end{aligned} \quad (12)$$

where

$$\mu_L = -\frac{r_j}{(r_j^2 + r_L^2)^{1/2}}, \quad (13)$$

and

$$\mu_{L1,2} = -\frac{r_j}{(r_j^2 + \xi_{1,2}^2)^{1/2}}. \quad (14)$$

Here the fraction f^{IC} is also given by Eqs. (8) and (9), while μ_j^s is given by

$$\mu_j^s = \frac{r_j}{(r_j^2 + r_d^2)^{1/2}}. \quad (15)$$

The electron density, $n_e(r_j) \sim r_j^{-2}$, for a relativistic jet as required by the mass conservation along the jet. The optical depth

$$\begin{aligned} \tau_{es}(r_j, r'_j) &= \cos^{-1} \theta_d(r'_j) \int_{r'_j}^{r_j} n_e(r_j) \sigma_T R_g dr_j, \\ &= \frac{\dot{M}_{jet} \sigma_T R_g}{4\pi m_e (1 - \cos \phi_j) R_g^2 c \cos \theta_d(r'_j) \beta_j \gamma_j} \left(\frac{1}{r_j} - \frac{1}{r'_j} \right), \end{aligned} \quad (16)$$

where

$$\cos \theta_d(r'_j) = \frac{r'_j \cos \phi_j}{[(r_d - r'_j \sin \phi_j)^2 + r'_j^2 \cos^2 \phi_j]^{1/2}}. \quad (17)$$

The occultation by the Compton thick part of the jet is considered, so the lower integral limit of Eq. (12) is given by $r'_{j,min} = \max(r_{j,tr}, r'_{j,min}^X)$, and

$$\begin{aligned} r'_{j,min}^X &= [\sin^2 \phi_j \cos^2 \theta_d^m(r_j) + \cos^2 \phi_j - \cos^2 \theta_d^m(r_j)]^{1/2} \\ &\times \frac{-r_d \sin \phi_j \cos^2 \theta_d^m(r_j) + r_d \cos \theta_d^m(r_j)}{\cos^2 \phi_j - \cos^2 \theta_d^m(r_j)}, \end{aligned} \quad (18)$$

where

$$\cos \theta_d^m(r_j) = \frac{r_j \cos \phi_j}{[r_j^2 \cos^2 \phi_j + (r_j \sin \phi_j + r_d)^2]^{1/2}}. \quad (19)$$

The total photons scattered by the jet that can photo-ionize the line-emitting disk region is

$$\frac{dN_{Comp}^{\text{line}}}{dt} = \begin{cases} \int_{r_{j,min}}^{r_{j,tr}} \frac{dN_{Comp}^{\text{line}}(r_j; r_j \leq r_{j,tr})}{dr dr_j} dr_j + \int_{r_{j,tr}}^{\infty} \frac{dN_{Comp}^{\text{line}}(r_j; r_j > r_{j,tr})}{dr dr_j} dr_j, & \text{if } r_{j,min} < r_{j,tr}, \\ \int_{r_{j,min}}^{\infty} \frac{dN_{Comp}^{\text{line}}(r_j; r_j > r_{j,tr})}{dr dr_j} dr_j, & \text{if } r_{j,min} \geq r_{j,tr}. \end{cases} \quad (20)$$

We can roughly estimate the luminosity of H α line emitted from the disk region between ξ_1 and ξ_2 by

$$L_{H\alpha} \sim h \nu_{H\alpha} \frac{dN_{Comp}^{\text{line}}}{dt}, \quad (21)$$

if the line emitting portion is photo-ionized by the X-ray photons scattered in the jet and the thermalization is not important.

We can derive $n_e(r_j)$ from Eqs. (2), and (3), if the ratio $L_{\text{kin}}/L_{\text{Edd}}$ is specified. Using Eqs. (2), (11), (12), (20) and (21), we can calculate $L_{H\alpha}/L_{\text{disk}}$ as a function of $L_{\text{kin}}/L_{\text{Edd}}$, when γ_j , $\gamma_{e,\min}$, and α_e are specified.

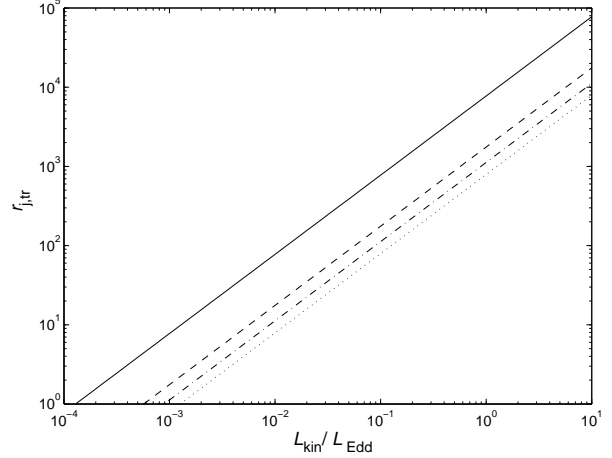


FIG. 2.— The radii $r_{j,tr}$ of the jets transit from Compton thick to Compton thin as functions of $L_{\text{kin}}/L_{\text{Edd}}$ for different values of $\gamma_j = 1.01$ (solid), 1.2 (dashed), 1.5 (dash-dotted), and 2 (dotted), respectively.

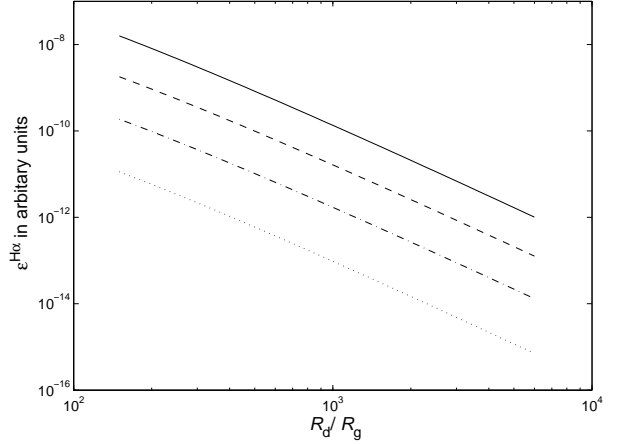


FIG. 3.— The emissivities $\epsilon^{H\alpha}$ as functions of disk radius R_d/R_g for different values of $\gamma_j = 1.2$ (solid), 1.5 (dashed), 2 (dash-dotted) and 3 (dotted), respectively.

4. TESTING THE MODEL

In this paper, we use the sample of RL AGNs with double-peaked broad lines given by Eracleous & Halpern (2003) to test our model. There are 20 sources with detected double-peaked H α lines in this sample (see Table 7 in their paper, and references therein). The bolometric luminosity is derived from soft X-ray luminosity. They found that the viscous power output W_d of the line-emitting disk region is insufficient for the observed H α luminosity for these sources, of which seven sources even have $W_d < L_{H\alpha}$. We list the bolometric and H α luminosities in Table 1 (converted to the cosmology adopted in this paper).

We estimate the jet power of these sources from their low-frequency radio emission. The relation between jet power and radio luminosity proposed by Willott et al. (1999) is

$$Q_{\text{jet}} \simeq 3 \times 10^{45} f^{3/2} L_{151}^{6/7} \text{ erg s}^{-1}, \quad (22)$$

where L_{151} is the total radio luminosity at 151 MHz in units of $10^{28} \text{ W Hz}^{-1} \text{ sr}^{-1}$. Willott et al. (1999) have argued that the normalization is uncertain and introduced the factor f to account for these uncertainties. They use a wide variety of arguments to suggest that $1 \leq f \leq 20$. Blundell & Rawlings

(2000) argued that $f \sim 10$ is a likely consequence of the evolution of magnetic field strengths as radio sources evolve. In this paper, we adopt $f = 10$ in all our calculations.

Finally, we need to estimate the masses of the black holes in these double-peaked line emitters. It is still unclear whether the empirical relation between the BLR size and optical continuum luminosity suggested by Kaspi et al. (2000) still holds for these AGNs (Wang et al. 2005; but also see Wu & Liu 2004), because the double-peaked lines are assumed to originate from accretion disks, which is different from the conventional cloud models for BLRs. In this paper, we use the relation between host galaxy absolute magnitude M_R at R-band and black hole mass M_{bh} proposed by McLure & Dunlop (2004),

$$\log_{10}(M_{\text{bh}}/\text{M}_{\odot}) = -0.50(\pm 0.02)M_R - 2.75(\pm 0.53), \quad (23)$$

to estimate the black hole masses. There are seven sources in this sample, of which the host galaxy magnitudes are unavailable in literature. We adopt the total magnitudes (including the nuclear emission), which may over-estimate the black hole masses for these seven sources.

In this work, we adopt $\phi_j = 1/\gamma_j$ for a free jet (Blandford & Königl 1979; Hutter & Mufson 1986), which is a good approximation even for a slow jet with $\gamma_j \sim 1$. Celotti & Fabian (1993) have argued that the lower energy cut for the non-thermal distributed relativistic electrons in the jets can be as low as $\gamma_{e,\text{min}} \sim 1$. Our model calculations are carried out for $\gamma_{e,\text{min}} = 1$. The spectral index for optically thin synchrotron radiation $\alpha_e = 0.75$ is adopted for all calculations in this work, which is consistent with observations on radio-loud AGNs (e.g., Jiang et al. 1998). The model calculations can be carried out, if the integral limits: $r_{j,\text{min}}$, ξ_1 , and ξ_2 are specified. In all our calculations, $r_{j,\text{min}} = 10$ is adopted. In Fig. 2, we show how the transition radius $r_{j,\text{tr}}$ of the jet from Compton thick to Compton thin varies with jet kinetic luminosity L_{kin} . The transition radius $r_{j,\text{tr}}$ increases with L_{kin} . The jet can be Compton thin down to $r_{j,\text{min}}$, when $L_{\text{kin}}/L_{\text{Edd}} \lesssim 10^{-3} - 10^{-2}$. For the cases with high kinetic luminosity $L_{\text{kin}}/L_{\text{Edd}}$, the jet is Compton thick even at very a large radius r_j . We integrate Eq. (20) over r_j (from $r_{j,\text{min}} = 10$) to calculate the emissivities $\epsilon^{\text{H}\alpha}$ as functions of radius in Fig. 3 for different values of γ_j . The final results depend insensitively on the value of $r_{j,\text{min}}$, because the solid angle of the outer line-emitting region subtended to the jet is very small if r_j is small. It is found that the emissivities have nearly power-law r -dependent distributions: $\propto r_d^{-\beta}$, and the values of β are ~ 2.5 . This implies that the ratio $L_{\text{H}\alpha}/L_{\text{disk}}$ is mainly governed by the inner radius ξ_1 of the line-emitting disk region. We integrate Eq. (20), and the relations between $L_{\text{kin}}/L_{\text{Edd}}$ and $L_{\text{H}\alpha}/L_{\text{disk}}$ are plotted in Fig. 4 for different values of γ_j . The data of the sample are plotted in the same figure for comparison.

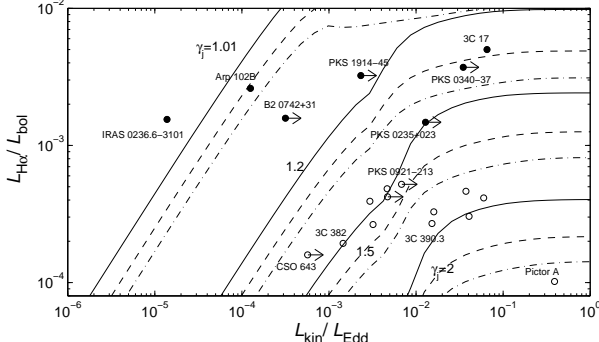


FIG. 4.— The relations between $L_{\text{kin}}/L_{\text{Edd}}$ and $L_{\text{H}\alpha}/L_{\text{bol}}$ for different values of γ_j . The lower electron energy cutoff $\gamma_{e,\text{min}} = 1$ is adopted in the calculations. The solid lines represent the line-emitting region extending from $\xi_1 = 200$ to $\xi_2 = 3000$ (the dashed lines are for $\xi_1 = 400$ and $\xi_2 = 3000$; the dash-dotted lines are for $\xi_1 = 600$ and $\xi_2 = 3000$). The filled circles represent the sources with $W_d < L_{\text{H}\alpha}$.

5. DISCUSSION

In the ion-supported torus scenario, the torus is truncated to a thin disk at a radius $R_{d,\text{tr}}$, and the X-ray photons from the torus are thought to illuminate the outer line-emitting disk region. The most favorable candidate for such an ion-supported hot torus is the RIAF (Narayan & Yi 1994, 1995). However, some double-peaked emitters have very luminous X-ray emission, which cannot be reproduced solely by the RIAFs in these sources if a reasonable viscosity parameter is adopted (see discussion in §2). It is quite doubtful whether RIAFs are in these X-ray luminous double-peaked line emitters. In Fig. 1, we find that most energy is radiated in the inner edge of the RIAF (more than 70 per cent of the total radiation of the RIAF is emitted from the region $R_d \lesssim 0.3R_{d,\text{tr}}$). Our calculation shows that less than 2.3 per cent radiation from the RIAF in the inner region of the disk can illuminate the outer disk region with $R_d \geq R_{d,\text{tr}}$ (see §2), which implies that the radiation of RIAFs is unable to solve the energy budget problem for most sources even if all the observed luminous X-ray emission in some double-peaked line emitters can be attributed to RIAFs.

Comparison between jet power estimated from the extended radio emission and kinetic luminosity of the jet requires $\gamma_{e,\text{min}} \sim 1$ for electron-positron jets, and $\gamma_{e,\text{min}} \sim 100$ for electron-proton jets (e.g., Celotti & Fabian 1993). For electron-proton jets, the inverse-Compton scattered photons by the electrons in the jet are in hard X-ray/γ-ray bands, which are inefficient for photo-ionizing the line-emitting disk region. In our present model, the line-emitting disk region is assumed to be irradiated by the scattered X-ray photons from the electron-positron jet. Most photons Compton up-scattered by the electrons in the electron-positron jets are in the soft X-ray band, which can efficiently photo-ionize the outer line-emitting disk region. Our calculations show that the jet can be Compton thin down to $r_{j,\text{tr}}$ if the jet kinetic luminosity $L_{\text{kin}}/L_{\text{Edd}}$ is low, while it can be Compton thick even at very large radii for high values of $L_{\text{kin}}/L_{\text{Edd}}$, because much matter is loaded by the jet with high $L_{\text{kin}}/L_{\text{Edd}}$. In our calculations, the minimal radius of the jet $r_{j,\text{min}} = 10$ is adopted. In principle, we can calculate the cases for a jet down to a radius lower than $r_{j,\text{min}} = 10$, though it is still unclear whether the Königl's conical jet is still valid to a very small radius near the black hole. Fortunately, the photons scattered near the bottom of the jet cannot photo-ionize the outer line-emitting disk region efficiently, because of the small solid angle subtended to the line-emitting region, which is similar to the RIAF case as discussed in §2. Thus, the final results have not been affected much even if a value of $r_{j,\text{min}} < 10$ is adopted.

In Fig. 3, we find that the emissivities $\epsilon^{\text{H}\alpha}$ have similar power-law r -dependence for different Lorentz factors γ_j adopted. We find $\epsilon^{\text{H}\alpha}$ varies with r nearly $\propto r^{-2.5}$ along the disk radius for all cases. The model fittings on the observed double-peaked line profile requires a power-law line emissivity with an index of $\sim 2 - 3$ for different sources (e.g., Chen & Halpern 1989; Chen et al. 1989; Eracleous & Halpern 1994, 2003), which is consistent with our model calculations. It is found that the emissivity de-

creases rapidly with increasing the Lorentz factor γ_j . For given jet kinetic luminosity, a higher γ_j leads to lower electron density (see Eqs. 2 and 3), which decreases the inverse-Compton scattered photons from the jet, and then the emissivity $\epsilon^{H\alpha}$.

The ratios $L_{H\alpha}/L_{\text{disk}}$ varying with $L_{\text{kin}}/L_{\text{Edd}}$ for different values of γ_j are plotted in Fig. 4. We plot the data of the sample in Fig. 4 to test our model by comparison with the model calculations. We find that the Lorentz factors of the jets $\gamma_j \lesssim 2$ are required to explain the observed data for most sources in this sample. The apparent angular velocity of the brightest jet component in 3C390.3 measured by VLBI is ~ 0.54 mas/year (Kellermann et al. 2004). The Lorentz factor of the jet in this source $\gamma_j \sim 2.1$ is therefore derived from its inclination angle $i = 26^\circ$, which is estimated from the fitting of its double-peaked line profile by Eracleous & Halpern (1994). In Fig. 4, one can find that a jet with $\gamma_j \sim 1.5 - 2$ is required by the model calculation for this source. For this source, $W_d \simeq 4.6L_{H\alpha}$ (Eracleous & Halpern 2003), which means that the Balmer line emission may be partly attributed to the local viscous heating of the line-emitting disk region, so our result is roughly consistent with that derived from the VLBI observations. Only one source, Pictor A, a jet with relatively larger Lorentz factor $\gamma_j > 2$ is required to illuminate the line-emitting region. This is a powerful radio galaxy (e.g., Wilson et al. 2001), and X-ray jet emission is detected in this source (Hardcastle 2005). The X-ray emission from the jet is important for this source, and the accretion disk luminosity derived from its X-ray luminosity is obviously overestimated, so the location of this source in Fig. 4 should be shifted upwards. A mild relativistic jet may probably provide sufficient scattered photons for photo-ionizing the line-emitting disk region in this source, if the X-ray emission is dominantly from the jet. For Arp 102B, a very low $\gamma_j \sim 1.01$ ($\sim 0.14c$) is required (see Fig. 4), i.e., a slowly moving conical outflow is present in this source, which is consistent with its compact radio structure (Biermann et al. 1981; Puschell et al. 1986; Caccianiga et al. 2001). Another special source, IRAS 0236.6-3101, which is difficult to be explained by this model (see Fig. 4). This is a star-forming galaxy with very weak radio emission (9.5 mJy at 1.4 GHz), and it probably has no jet. The origin of its double-peaked lines may be similar to that of radio-quiet double-peaked line emitters, which will be addressed in the last paragraph of this section.

For the seven sources with only upper limits on black hole masses (lower limits on the ratios $L_{\text{kin}}/L_{\text{Edd}}$), they are similar to others and the jets with moderate Lorentz factors $\gamma_j \lesssim 2$ can solve the “energy budget” problem. As the detailed model fittings for individual sources indicate that the line-emitting regions in these sources have different sizes (see Eracleous & Halpern 2003, for details), our calculations have been carried out for different values of ξ_1 and ξ_2 (see different line types in Fig. 4), which have not altered our main conclusion.

There are 13 sources in this sample with $W_d/L_{H\alpha} > 1$. Although it means the local viscous power in the line-emitting disk regions may be sufficient for the line emission for these 13 sources, the temperatures of the line-emitting disk portions are still too low for all the observed $H\alpha$ line emission. The external illuminating from the jets is still necessary for these sources. In our model, an electron-positron jet is required to scatter disk photons back to photo-ionize the outer disk surface to produce Balmer lines. We suggest that future VLBI polarization observations on these radio-loud double-peaked

line emitters can test this model.

In this paper, some quantities, M_{bh} , L_{bol} , and L_{kin} , are derived from observed quantities by using the conventional approaches reported in literature, of which the uncertainties might affect our results. However, the qualitative conclusion that slow jets/outflows are required in double-peaked emitters would not be altered (see Fig. 4), for typical errors for these quantities, i.e., a factor of ~ 3 for M_{bh} , and the derived kinetic luminosity L_{kin} is accurate at an order of magnitude. In our present calculation of $L_{H\alpha}$, we have not included the thermalization of the disk. If the thermalization is considered, the resulted $L_{H\alpha}$ will become lower, so a lower bulk Lorentz factor γ_j of the jet than our present model calculation is required (see Fig. 4).

Besides radio-loud AGNs in this sample, several ten radio-quiet double-peaked line emitters have been discovered (Strateva et al. 2003). Although no jet is present in these radio-quiet AGNs, we speculate that slow moving outflows may be in these sources, which play the same role of the jets in their radio-loud counterparts. If the electrons in the outflows are non-relativistic, a fraction of disk power radiated from its inner region can be Thomson scattered to the outer line-emitting portion of the disk. If the Thomson scattering depth is ~ 0.2 , the outflows can scatter nearly one-tenth of the disk radiation to illuminate the outer line-emitting disk portion. If this is the case, the absorption by the outflows in these radio-quiet AGNs is expected to be detected by X-ray observations, which can be a test on our model. The lack of detected double-peaked broad emission lines in strong radio-loud quasars with relativistic jets is a natural prediction of our model, i.e., the Compton scattering power is too weak to irradiate the outer line-emitting portion for fast moving jets. For radio-quiet AGNs, only those having outflows with suitable scattering depth can scatter disk photons back to illuminate the outer line-emitting portion, which leads to double-peaked broad emission lines. Recent X-ray observations showed that a fraction of quasars and Seyfert galaxies have X-ray absorption with column density $\gtrsim 10^{23} \text{ cm}^{-3}$ (e.g., Reeves et al. 2003; Young et al. 2005; Piconcelli et al. 2005), which implies that the AGNs having outflows with suitable scattering depth ~ 0.2 are not common among all AGNs. However, it does not mean that all AGNs with suitable scattering depth will exhibit double-peaked lines. Some other factors, such as, the viewing angle and the properties of the accretion disk, may play important roles in producing double-peaked lines. The quantitative model calculations to fit the line profiles for individual AGNs are beyond the scope of this work, which will be reported in the forthcoming paper.

In this work, we suggest that the soft photons scattered by electrons in electron-position jets for radio-loud double-peaked line emitters (or in slow outflows with suitable scattering depth for radio-quiet counterparts) can efficiently ionize the line-emitting disk regions. Another possibility is that slow outflows play the same role in radio-loud double-peaked line emitters as radio-quiet sources, though it is still unclear whether relativistic jets can co-exist with such cold outflows in radio-loud double-peaked line emitters. However, it is unable to explain the fact that no double-peaked emission line is present in strong radio quasars with relativistic jets, while this is a natural prediction of the electron-positron jet model proposed in this work.

gestions. This work is supported by the National Science Fund for Distinguished Young Scholars (grant 10325314),

and the NSFC (grant 10333020).

REFERENCES

Antonucci, R. 1993, *ARA&A*, 31, 473
 Armitage P.J. 1998, *ApJ*, 501, L189
 Biermann, P., Preuss, E., Kronberg, P. P., Schilizzi, R. T., & Shaffer, D. B. 1981, *ApJ*, 250, L49
 Blandford, R. D., & Königl, A. 1979, *ApJ*, 232, 34
 Blundell, K.M., & Rawlings, S. 2000, *AJ*, 119, 1111
 Caccianiga, A., March? M. J. M., Thean, A., & Dennett-Thorpe, J. 2001, *MNRAS*, 328, 867
 Cao, X., 2005, *ApJ*, 631, L101
 Celotti, A., & Fabian, A. C. 1993, *MNRAS*, 264, 228
 Chen, K., & Halpern, J. P. 1989, *ApJ*, 344, 115
 Chen, K., Halpern, J. P., & Filippenko, A. V. 1989, *ApJ*, 339, 742
 Dumont, A. M., & Collin-Souffrin, S. 1990, *A&A*, 229, 313
 Dunlop, J. S. et al. 2003, *MNRAS*, 340, 1095
 Eracleous, M., & Halpern, J. P. 1994, *ApJS*, 90, 1
 Eracleous, M., & Halpern, J. P. 2003, *ApJ*, 599, 886
 Falomo, R., Carangelo, N., & Treves, A. 2003, *MNRAS*, 343, 505
 Freeman, K. C., et al. 1977, *A&A*, 55, 445
 Fukugita, M., Shimasaku, K., & Ichikawa, T. 1995, *PASP*, 107, 945
 Gaskell, C. M. 1983, in *Quasars and gravitational lenses: Proceedings of the Twenty-fourth Liege International Astrophysical Colloquium*, Belgium, Universite de Liege, p473
 Gaskell, C. M. 1988, in *Active Galactic Nuclei*. Proceedings of a conference held at the Georgia State University, Atlanta, Georgia, Eds. Miller, H. R., & Wiita, P. J., Publisher, Springer-Verlag, Berlin, p61
 Goad, M., & Wanders, I. 1996, *ApJ*, 469, 113
 Hardcastle, M. J. 2005, *MNRAS*, in press, (astro-ph/0511511)
 Hawley, J.F., & Balbus, S.A. 2002, *ApJ*, 573, 738
 Hutter, D. J., & Mufson, S. L. 1986, *ApJ*, 301, 50
 Jiang, D.R., Cao, X., & Hong, X.Y. 1998, *ApJ*, 494, 139
 Kaspi, S., Smith, P.S., Netzer, H., Maoz, D., Jannuzzi, B.T., & Giveon, U. 2000, *ApJ*, 533, 631
 Kellermann, K. I. et al., 2004, *ApJ*, 609, 539
 Königl, A. 1981, *ApJ*, 243, 700
 Lauberts, A., & Valentijn, E. A. 1989, *The Surface Photometry Catalogue of the ESO-UPPSALA galaxies*, Garching bei Munchen: European Southern Observatory
 Manmoto, T., 2000, *ApJ*, 534, 734
 McLure, R.J., & Dunlop, J.S. 2001, *MNRAS*, 327, 199
 McLure, R.J., & Dunlop, J.S. 2004, *MNRAS*, 352, 1390
 Narayan, R., & Yi, I. 1994, *ApJ*, 428, L13
 Narayan, R., & Yi, I. 1995, *ApJ*, 444, 231
 Pagani, C., Falomo, R., & Treves, A. 2003, *ApJ*, 596, 830
 Perez, E., Mediavilla, E., Penston, M. V., Tadhunter, C., & Moles, M. 1988, *MNRAS*, 230, 353
 Piconcelli, E. et al., 2005, *A&A*, 432, 15
 Puschell, J. J., Moore, R., Cohen, R. D., Owen, F. N., & Phillips, A. C. 1986, *AJ*, 91, 751
 Reeves, J. N., O'Brien, P. T., & Ward, M. J., 2003, *ApJ*, 593, L65
 Renaud, N., & Henri, G. 1998, *MNRAS*, 300, 1047
 Schneider, D. P., Schmidt, M., & Gunn, J. E. 1994, *AJ*, 107, 1245
 Shakura, N.I., & Sunyaev, R.A. 1973, *A&A*, 24, 337
 Smith, E. P., & Heckman, T. M., 1989, *ApJS*, 69, 365
 Stepanian, J. A. et al. 2001, *AJ*, 122, 3361
 Strateva, I. V., et al. 2003, *AJ*, 126, 1720
 Two Micron All Sky survey team, 2003, 2MASS extended objects, final release
 Wang, T.G., et al., 2005, *ApJ*, 625, L35
 Wardle, J. F. C., Homan, D. C., Ojha, R., & Roberts, D. H., 1998, *Nat*, 395, 457
 Willott, C.J., Rawlings, S., Blundell, K.M., & Lacy, M. 1999, *MNRAS*, 309, 1017
 Wilson, A. S., Young, A. J., & Shopbell, P. L. 2001, *ApJ*, 547, 740
 Worrall, D.M., & Birkinshaw, M., 2004, astro-ph/0410297
 Wu, X. -B., & Liu, F. K. 2004, *ApJ*, 614, 91
 Zheng, W., Sulentic, J. W., & Binette, L. 1990, *ApJ*, 365, 115
 Zirbel, E. L. 1996, *ApJ*, 473, 713
 Young, A. J. et al., 2005, *ApJ*, 631, 733

TABLE 1
DATA OF THE SAMPLE

Source name	redshift	$\log_{10} M_{\text{bh}}/\text{M}_{\odot}$	reference	$\log_{10} L_{\text{H}\alpha}$	$\log_{10} L_{\text{bol}}$	$\log_{10} Q_{\text{jet}}$	$L_{\text{H}\alpha}/L_{\text{bol}}$	$Q_{\text{jet}}/L_{\text{Edd}}$
3C 17	0.220	8.81 ^a	1	43.50	45.80	45.73	5.0×10^{-3}	5.92×10^{-2}
4C 31.06	0.373	9.66 ^a	2	43.08	46.66	45.17	2.65×10^{-4}	2.91×10^{-3}
3C 59	0.109	8.59	3	42.82	46.30	44.89	3.28×10^{-4}	1.45×10^{-2}
PKS 0235+023	0.209	<8.91 ^a	4	43.85	46.68	44.95	1.48×10^{-3}	7.87×10^{-3}
IRAS 0236.6-3101	0.062	8.83	5	42.20	45.01	42.07	1.55×10^{-3}	1.25×10^{-5}
PKS 0340-37	0.285	<8.87	2	44.22	46.65	45.50	3.71×10^{-3}	3.16×10^{-2}
3C 93	0.357	8.99	6	43.20	46.59	45.86	4.14×10^{-4}	5.43×10^{-4}
MS 0450.3-1817	0.059	7.63 ^b	7	41.28	44.69	43.20	3.91×10^{-4}	2.68×10^{-3}
Pictor A	0.035	7.62 ^a	8	41.77	45.76	45.31	1.02×10^{-4}	3.53×10^{-1}
B2 0742+31	0.462	<11.22 ^a	9	44.63	47.43	45.81	1.58×10^{-3}	2.87×10^{-4}
CBS 74	0.092	<8.73 ^a	2	42.92	46.29	44.50	4.22×10^{-4}	4.28×10^{-3}
PKS 0921-213	0.053	<7.87 ^a	2	42.42	45.70	43.80	5.21×10^{-4}	6.19×10^{-3}
PKS 1020-103	0.197	8.85	10	43.54	46.86	44.61	4.83×10^{-4}	4.23×10^{-3}
CSO 643	0.276	<9.77 ^a	11	43.25	47.05	44.62	1.59×10^{-4}	5.16×10^{-4}
3C 303	0.141	8.27 ^a	8	42.29	45.81	44.97	3.04×10^{-4}	3.269×10^{-2}
3C 332	0.151	8.53 ^a	8	42.46	45.79	45.20	4.63×10^{-4}	3.40×10^{-2}
Arp 102B	0.024167	8.34	12	41.87	44.46	42.54	2.61×10^{-3}	1.14×10^{-4}
3C 382	0.05787	9.38 ^a	1	43.07	46.78	44.64	1.93×10^{-4}	1.32×10^{-3}
3C 390.3	0.0561	8.59	13	42.57	46.14	44.87	2.69×10^{-4}	1.38×10^{-2}
PKS 1914-45	0.368	<10.37 ^a	9	43.75	46.24	45.83	3.23×10^{-3}	2.11×10^{-3}

REFERENCES. — (1) Smith & Heckman (1989); (2) Eracleous & Halpern (2003); (3) McLure & Dunlop (2001); (4) Schneider (1994); (5) Lauberts & Valentijn (1989); (6) Pagani et al. (2003); (7) Two Micron All Sky survey team (2003); (8) Zirbel (1996); (9) NED; (10) Falomo et al. (2003); (11) Stepanian et al. (2001); (12) Freeman et al. (1977); (13) Kaspi et al. (2000).

NOTE. — Column (3) the black hole mass is estimated from the host galaxy R-band magnitude except the two sources: Arp 102B and 3C390.3; Columns (5)–(7) in units of erg s^{-1} :

^aThe R-band magnitude is converted from V-band magnitude assuming $m_V - m_R = 0.61$ (Fukugita et al. 1995).

^bThe R-band magnitude is converted from K-band magnitude assuming $m_R - m_K = 2.5$ (Dunlop et al. 2003).